Scripta Materialia 137 (2017) 119–122

Contents lists available at ScienceDirect

Scripta Materialia

journal homepage: www.elsevier.com/locate/scriptamat

Regular article

The role of indenter radius on spherical indentation of high purity magnesium loaded nearly parallel to the c-axis

Ghazal Nayyeri [a,*], Warren J. Poole [a], Chad W. Sinclair [a], Stefan Zaefferer [b]

[a] University of British Columbia, Vancouver, BC, Canada
[b] Max-Planck Institute for Iron Research, Dusseldorf, Germany

ARTICLE INFO

Article history:
Received 1 April 2017
Received in revised form 27 April 2017
Accepted 27 April 2017
Available online xxxx

Keywords:
Magnesium
Indentation size effect
Critical resolved shear stress (CRSS)

ABSTRACT

The current work proposes two main contributions based on a study of the effect of indenter radius on spherical indentation of magnesium where loading is nearly parallel to the c-axis. First, it is illustrated that high purity magnesium shown a strong indentation size effect for spherical indentation. The CRSS for basal slip and extension twinning are estimated by extrapolation of the RSS data for an infinitely large indenter radius. Second, it is shown that the number of twins which de-twin during unloading depends on the indenter size, indentation depth, and the magnitude of the plastic strain and stress under the indenter.

Indentation testing offers an attractive technique to extract information on the basic plastic deformation mechanisms operating during the indentation of magnesium. The response of magnesium depends sensitively, however, on factors such as i) the indenter shape (e.g. [1,2], spherical [3–5], sphero-conical [6,7], cube-corner [8]) ii) the crystallographic orientation of the loading axis [6,8,9], iii) the penetration depth of the indenter [1,4] and iv) the size of the indenter [1–3,5,9,10]. The dependence on indenter size and penetration is normally accounted for in FCC metals by the indentation size effect (ISE), which has been interpreted in terms of the local strain gradient developed in the deformation zone under the indent [11–30]. However, there is relatively little data available on the indentation size effect for magnesium.

There have been few attempts to extract the critically resolved shear stresses (CRSS) for slip from spherical indentation of magnesium. Catoor et al. [5] and Nayyeri et al. [34], examined the onset of plasticity during indentation parallel to [0001] with 3.3 μm, and 13.3 μm radius spherical indenters, respectively. Comparing the results, it can be seen that the CRSS for basal slip is strongly dependent on indenter radius, i.e. Catoor et al. reported 600–1200 MPa [5] while Nayyeri et al. found 66 MPa [31]. Further, Guo observed that the CRSS for basal slip in AZ31B increased from 100 to 380 MPa as the radius of the spherical indenter was decreased from 50 to 5 μm, again suggesting a significant size dependence [32]. Given these results, the current study was conducted to systematically characterize the effect of indenter radius for loading nearly parallel to the [0001] direction in magnesium.

The material studied in this work is commercially pure magnesium (~99.98 wt% Mg) supplied by US Magnesium LLC. Spherical indentation tests were conducted using indenters of radii, 1.0, 3.0, 13.3, 50 and 250 μm to three different depths (500 nm, 1500 nm, and 3500 nm) on a single large grain (grain size approximately 1 mm) within a polycrystalline magnesium sample. The angle between the indentation loading direction and the c-axis was 9.3° as determined by EBSD, i.e. nearly parallel to [0001]. An MTS XP Nanoindenter was employed with a loading rate of 5 mN/s and a data acquisition rate of 15 Hz. The method of Kalidindi and Pathak was used to determine the zero-load and zero-displacement point [33]. Samples were prepared by polishing to a 1 μm diamond finish followed by chemical polishing in a solution of 10% nitric acid in 90% absolute ethanol for 5 min. Finally, the samples were electro-polished using 20% nitric acid in absolute ethanol cooled to −20 °C at a voltage of 20–30 V. Three-dimesional EBSD-based orientation microscopy observations were conducted after indentation using a Zeiss XB 1540 dual-beam high-resolution field emission scanning electron microscope equipped with an Orsay Physics focused ion beam (FIB) column. An EDAX/TSL EBSD system was used to measure the EBSD maps. The 3D EBSD data sets were acquired by serial sectioning of a block of material containing the indent and placed close to the corner of the sample (see references [34,35] for more detail).

Fig. 1a displays the overall indentation load-displacement curve, alongside the Hertzian prediction (red line), from a test using an indenter with a 13.3 μm radius [36,37]. Fig. 1b shows an enlarged view of the loading where one can observe six discontinuities prior to a depth of 500 nm. It has been proposed that the initial deviation from elastic Hertz Law behaviour is associated with the onset of plasticity [3,35] by the easiest deformation mode, in this case ⟨a⟩ dislocations on the basal

* Corresponding author.
E-mail addresses: g.nayyeri@gmail.com (G. Nayyeri), warren.poole@ubc.ca (W.J. Poole), Chad.Sinclair@ubc.ca (C.W. Sinclair), s.zaefferer@mpie.de (S. Zaefferer).

http://dx.doi.org/10.1016/j.scriptamat.2017.04.039
1359-6462/

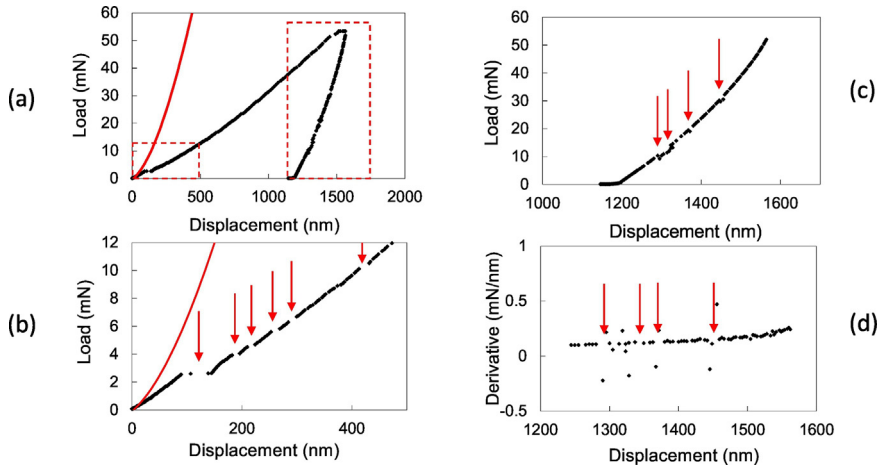

Fig. 1. (a) The load-displacement curve for indent depth of 1500 nm, a magnified view of (b) the loading curve, and (c) the unloading curve and (d) the derivative of the unloading curve. (For interpretation of the references to colour in this figure, the reader is referred to the web version of this article.)

plane. Continued indentation requires the activation of $(1\,0\,\bar{1}\,2)$ extension twins so as to allow for material to flow outwards under the indenter and upwards to the surface [35].

To examine the stress at which basal slip is initiated, indentation stress-strain curves were obtained from the load-displacement data using the method of Kalidindi and Pathak [33]. Fig. 2a illustrates the indentation stress-strain curves for indenters having radii of 1.0, 3.0, 13.3, 50 and 250 μm. Table 1 summarizes the indentation yield stress obtained assuming a 0.1% offset for the 5 tests with different indenter radii. An 'effective' Schmid factor of 0.36 was found from resolving the stress state under the indenter (assuming Hertz Law [38]) onto the basal plane for this crystal orientation. The resolved shear stress (RSS) at the onset of plasticity calculated using this value of the Schmid factor is shown in Table 1. It can be seen that the RSS at the onset of plasticity strongly increases as the indenter radius decreases i.e. from 21 to 250 MPa as the indenter radius decreases from 250 to 1 μm.

In order to rationalize this size dependence, it is useful to examine the pattern of deformation under the indenter. Fig. 3 shows one example of the misorientation profile measured by EBSD under the centre of an indent formed by an indenter with radius of 13.3 μm indented to a depth of 1500 nm. Note, the EBSD map of the centre cross-section slice has been shown in Fig. 6b of our previous work [35]. In Fig. 3, the misorientation angle with respect to the material far from the indent is plotted over the normalized distance to the centre of the indent at a depth of 8 μm under the indent. It can be observed that the misorientation angle abruptly increases to ≈10° at the left edge of the indent and then changes with a roughly constant slope until the right side of the indent is reached, where it abruptly returns to zero. Nayyeri et al., have shown, using 3D-EBSD reconstructions under the indent, that this misorientation gradient can be characterized as a rotation about $\langle 1\,1\,\bar{2}\,0\rangle$ or $\langle 1\,0\,\bar{1}\,0\rangle$ consistent what would be expected from an array of basal dislocations under the indent [35]. The gradient of misorientation with respect to the radial distance, r, from the centre of the indent, $\frac{d\theta}{dr}$, is found to be:

$$\frac{d\theta}{dr} = \frac{\theta_{max}}{a} \tag{1}$$

where θ_{max} is the maximum misorientation under the indenter (Fig. 3). The crystal plasticity finite element method calculations of Nayyeri et al. [35] showed that θ_{max} is a linear function of the ratio of the depth of the indent, h, to the indent contact radius, a, i.e. $\theta_{max} = Kh/a$, where K is a constant, and $a = \sqrt{2Rh}$ where R is the radius of the indenter [33]. Thus, $d\theta/dr$ can be expressed as:

$$\frac{d\theta}{dr} = \frac{Kh/a}{a} = K\frac{h}{2Rh} = \frac{K'}{R} \tag{2}$$

where $K' = K/2$.

The density of geometrically necessary dislocations, ρ, under the indent can be written in terms of the misorientation gradient, $d\theta/dr$ as:

$$\rho = \frac{1}{b}\frac{d\theta}{dr} \tag{3}$$

or substituting Eq. (2) with Eq. (3)

$$\rho = \frac{1}{b}\frac{K'}{R} \tag{4}$$

where b is the magnitude of the Burgers vector. It is proposed that the initial plastic flow of the material occurs by motion of basal dislocations on parallel planes under the indent. The maximum interaction stress between parallel segments of dislocations is inversely proportional to the

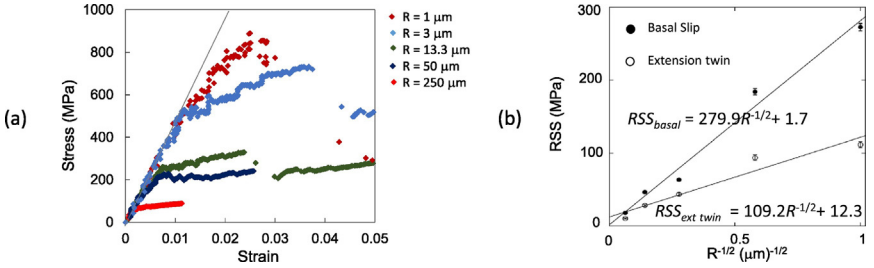

Fig. 2. (a) The indentation stress-strain curves using indenters of radii, 1, 3, 13.3, 50 and 250 μm, (b) the resolved shear stress (RSS) at the onset of plasticity vs. inverse square root of indenter radius for basal slip and extension twinning.